HHS Public Access

Author manuscript

Science. Author manuscript; available in PMC 2018 September 23.

Published in final edited form as:

Science. 2018 March 23; 359(6382): 1403–1407. doi:10.1126/science.aal3622.

Lymph node metastases can invade local blood vessels, exit the node and colonize distant organs in mice

Ethel R. Pereira[1], **Dmitriy Kedrin**[1,2], **Giorgio Seano**[1], **Olivia Gautier**[1,3], **Eelco F.J. Meijer**[1], **Dennis Jones**[1], **Shan-Min Chin**[1], **Shuji Kitahara**[1], **Echoe M. Bouta**[1], **Jonathan Chang**[4], **Elizabeth Beech**[1], **Han-Sin Jeong**[5], **Michael C. Carroll**[6], **Alphonse G. Taghian**[7], and **Timothy P. Padera**[1,*]

[1]Edwin L. Steele Laboratories, Department of Radiation Oncology, MGH Cancer Center, Massachusetts General Hospital, Boston, MA and Harvard Medical School, Boston, MA, USA

[2]Division of Gastroenterology Massachusetts General Hospital, Boston, MA and Harvard Medical School, Boston, MA, USA

[3]Department of Biological Engineering, Massachusetts Institute of Technology, Cambridge, MA, USA

[4]Graduate Program in Immunology, Division of Medical Sciences, Harvard Medical School, Boston, MA, USA and Program in Cellular and Molecular Medicine, Children's Hospital Boston, Boston, MA, USA

[5]Department of Otorhinolaryngology-Head and Neck Surgery, Samsung Medical Center, Sungkyunkwan University School of Medicine, Seoul, South Korea

[6]Department of Pediatrics, Harvard Medical School, Boston, MA, USA and Program in Cellular and Molecular Medicine, Children's Hospital Boston, Boston, MA, USA

[7]Department of Radiation Oncology, Massachusetts General Hospital, Boston, MA, USA

Abstract

Lymph node metastases in cancer patients are associated with tumor aggressiveness, poorer prognosis and the recommendation for systemic therapy. Whether cancer cells in lymph nodes can seed distant metastases has been a subject of considerable debate. We studied mice implanted with cancer cells (mammary carcinoma, squamous cell carcinoma or melanoma) expressing the photoconvertible protein Dendra2. This technology allowed us to selectively photoconvert metastatic cells in the lymph node and trace their fate. We found that a fraction of these cells invaded lymph node blood vessels, entered the blood circulation, and colonized the lung. Thus, in mouse models, lymph node metastases can be a source of cancer cells for distant metastases. Whether this mode of dissemination occurs in human cancer remains to be determined.

Solid tumor progression is characterized by metastasis to regional lymph nodes and dissemination to distant organs. The presence of lymph node disease in cancer patients

*Correspondence to: tpadera@steele.mgh.harvard.edu.

The authors declare no competing financial interests.

correlates with a poorer prognosis and dictates in part the course of treatment (1–5). However, there is a robust ongoing debate about the role of lymph node metastasis in further progression of disease (6, 7). Some experts contend that localized lymph node metastases are clinically inconsequential (8, 9), whereas others contend that lymph node metastases have the potential to seed distant organs (5, 10–12) and therefore should be treated to prevent distant metastasis (13, 14). This debate has taken on new urgency with the recent completion of clinical trials that suggest nodal dissection beyond the sentinel (first) lymph node does not provide therapeutic benefit to patients who have received adjuvant radiation therapy and systemic therapies (15–19). Other data show that radiation therapy of regional lymph nodes improves the outcome of patients with early-stage breast cancer (20, 21), suggesting that treatment of metastatic lymph nodes benefits a subgroup of patients (22, 23).

In this study, we used mouse models to investigate whether cancer cells exit the lymph node and disseminate to distant sites. We stably expressed the photoconvertible fluorescent protein Dendra2 (cytosolic localization) or Dendra2 fused to the nuclear protein histone H2B (Dendra2H2B-nuclear localization) in 4T1 murine mammary cancer cells (a model of triple-negative breast cancer), B16F10 murine melanoma cells and SCCVII murine squamous cell carcinoma cells. Dendra2 is a green-emitting fluorescent protein that can be converted to emit red light by exposure to 405nm light (24). Expression of Dendra2 in these cell lines did not affect cell migration, proliferation rates or *in vivo* tumor growth compared to parental lines (fig. S1). We orthotopically implanted tumor cells into syngeneic mice and resected the primary tumor once it reached a volume of ~250-500 mm^3. Next, we used a 405nm laser diode on 5 consecutive days to convert Dendra2H2B-cancer cells from green to red fluorescence, restricting the light exposure to the metastatic lymph node (Fig. 1A). Tissue clearing of the resected primary tumor revealed that no cancer cells at the primary site underwent spontaneous photoconversion (fig. S2). The *in vivo* photoconversion efficiency in the lymph node was 70% for 4T1 cells, 62% for B16F10 cells and 56% for SCCVII cells (fig. S3).

We next determined whether photoconverted circulating tumor cells (CTCs) appeared in the blood of animals that had undergone photoconversion of the lymph node. The presence of red fluorescent CTCs would show that these cells originated from lymph node metastases. We identified red photoconverted 4T1 CTCs and B16F10 CTCs (Fig. 1B, 1C and fig. S4A-B) that disseminated from the lymph node. CTCs from 4T1-Dendra2 and 4T1-Dendra2H2B lymph node metastasis were grown *in vitro* to confirm viability. Both viable red (lymph node origin) and green fluorescent CTCs were observed after 1 day in culture. By day 7, only green colonies formed as red fluorescence is lost as the photoconverted cells divide (fig. S4C). These data show that viable cancer cells from the lymph node have the potential to exit the node and survive in the blood. We did not detect photoconverted SCCVII CTCs (Fig. 1B and fig. S4D), although our methods could detect these cancer cells when photoconverted *in vitro* (fig. S5A) and in the lymph node of SCCVII tumor-bearing animals (fig. S5B).

To explore whether cancer cells that transited the lymph node can seed distant organs, we analyzed the lungs of mice after photoconversion of their metastatic lymph nodes. Confocal microscopy revealed the presence of isolated photoconverted (red) cancer cells in the lungs

of animals with 4T1 (Fig. 2A and 2B) and B16F10 cancers (Fig. 2C and 2D). Among the isolated cancer cells detected in the lung, 70% of 4T1 cells and 68% B16F10 cells were of lymph node origin (Fig. 2B and 2D). We performed a spectral scan from 426nm to 661nm with a 5nm bandwidth (fig. S6), which showed distinct signals for DAPI (emission spectra between 450/20nm), native Dendra2H2B (emission spectra between 507/10nm) and photoconverted Dendra2H2B (emission spectra between 572/10nm) (24) in lung sections, with no significant signal at other wavelengths. These data demonstrate the specificity of our detection methods to identify lung metastasis of lymph node origin. We did not detect cancer cells in the lungs of SCCVII bearing mice.

We next evaluated whether the primary tumor can also seed the lung directly without transiting the lymph node. By photoconverting 4T1-Dendra2H2B primary tumors only (fig. S7A), prior to their dissemination to lymph node (fig. S7B), we detected photoconverted CTCs (fig. S7C) in whole blood from these animals, which could only have originated from the primary tumor. Next, we prophylactically excised the sentinel lymph nodes from BALB/c mice (fig. S8) prior to injecting 4T1-DendraH2B cancer cells into the mammary fat pad (MFP). Two weeks after primary tumor resection, we detected CTCs and lung metastases in the absence of lymph nodes. However, animals with intact lymph nodes had higher numbers of CTCs and lung metastases compared to animals with lymph nodes removed (fig. S8). Taken together, these data show that cancer cells from the primary site can directly enter the systemic circulation and seed the lung.

We then examined whether both routes of metastasis—transit via the lymph node or transit directly from the primary tumor—can contribute to distant metastatic lesions. To this end, we injected Dendra2-expressing (green fluorescent protein) 4T1 cancer cells directly in the axillary lymph node (fig. S9A). On the contralateral side, the lymph node was removed one week prior to injection of mCherry-expressing (red fluorescent protein) 4T1 cancer cells into the MFP (Fig. 2E; fig. S9B). Ten days after resecting both the tumor bearing lymph node and MFP tumor, we detected both red and green lung metastases (Fig. 2F, H&E staining in fig. S9C). We measured a large variation in the ratio of green:red metastatic lung lesions across multiple animals (average ratio of 8 green:5 red metastatic lesions; Fig. 2G). Despite this large variation, every animal had lung metastases that originated from both lymph node lesions and directly from the primary tumor.

Cancer cells could take two possible routes to exit the lymph node and spread systemically — through lymph node blood vessels or efferent lymph. We hypothesized that cancer cells can escape the lymph node by directly invading lymph node blood vessels. Immunohistochemical analysis of 4T1 tumor draining lymph nodes revealed isolated cancer cells (cytokeratin positive) in close association with CD31-positive blood vessels, within high endothelial venules (HEVs) and breaching the vascular basement membrane (collagen IV positive) (Fig. 3A). In metastatic lymph nodes with only isolated cancer cells (fig. S10A), quantitative analysis showed that 23±2% of isolated cancer cells were within 5μm of a blood vessel, compared to only 11±1% using a model of randomly distributed cells in the lymph node (Fig. 3B-C, $p<0.05$). Further, 6±2% of the cancer cells were inside blood vessels (Fig. 3D, fig. S10B). A similar analysis performed in lymph nodes containing larger metastatic lesions (>200μm in diameter, fig. S11A) did not show this tropism (fig. S11B, $p>0.05$). As

metastatic lesions grow, the surface area of the blood vessels becomes limiting, causing the distribution of cancer cells to revert to that of a random distribution. This phenotype is consistent with the lack of sprouting angiogenesis in lymph node metastases (25). In lymph nodes with large lesions, 1%±0.5% of cancer cells were found in blood vessels (Fig. 3D). A similar analysis did not show an association between cancer cells and lymphatic vessels in tumor draining lymph nodes (fig S12, $p>0.05$).

We also analyzed lymph nodes with large metastatic lesions from 19 patients with head and neck cancer. Similar to large lesions in mouse lymph nodes, cancer cells in human lymph nodes did not demonstrate measurable tropism to blood vessels due to the limitation in vessel surface area. However, at the edge of the metastatic lesions we found cancer cells that were closely associated with blood vessels (fig. S13). In addition, we detected isolated cancer cells inside blood vessels in 6 of the 19 patient samples (fig. S13), consistent with our pre-clinical data.

To confirm that metastatic cancer cells in a lymph node have an affinity for lymph node blood vessels, we used time-lapse multiphoton intravital microscopy to measure cancer cell migration in an optical lymph node window in mice (25). Dendra2-expressing metastatic cancer cells are first seen in the subcapsular sinus and later invade the cortex of the lymph node. There, they accumulate around rhodamine-dextran labeled blood vessels (Fig. 4A-C, fig. S14) or associate with lymph node conduits, which contain a fibrillar collagen core surrounded by fibroblastic reticular cells (FRCs) (Fig. 4D). Cancer cells can be observed in directed migration toward blood vessels as well as moving inside blood vessels (Movies S1–3, Fig. 4E). Time-lapse imaging of tumor-draining lymph nodes revealed that only a small fraction of cancer cells in the lesion are motile. Both 4T1 and SCCVII cells that were motile had an average speed of 7μm/hour (Fig. 4F), similar to the speed of resident lymph node stromal cells such as FRCs, follicular dendritic cells, macrophages and resident dendritic cells (26). However, a greater fraction of 4T1 cells were motile compared to SCCVII cells (Fig. 4G). Consistent with our observations in tissue sections (Fig. 3F), cancer cells create persistent associations with blood vessels (Fig. 4B-C) as well as conduits (Fig. 4D). The conduit system is an interconnected collagen network formed by FRCs that creates pathways for dendritic cells to navigate through the lymph node to interact with naïve lymphocytes near high endothelial venules (27). We speculate that, similar to dendritic cells, cancer cells use the conduit system to aid in their migration to lymph node blood vessels.

The Dendra2 system has limitations. First, the photoconversion of the green Dendra2 protein to red fluorescence can only be detected for 5-6 days before the cells appear green again. Second, the photoconversion efficiency of Dendra2H2B in the lymph node was ~60-70% in our tumor models. Thus, in mice that underwent photoconversion of metastatic cancer cells in the lymph node, green-Dendra2H2B-expressing cancer cells in the blood or lungs could have multiple sources, including from the primary tumor directly, from unconverted cancer cells in the lymph node or from photoconverted cancer cells in the lymph node that lost their red fluorescence with cell division. These limitations prevent us from accurately assessing what percentage of distant metastases originates from lymph node metastases.

The absence of detectable photoconverted CTC's and lung metastasis in the SCCVII cancer model, reflects the variability in the aggressiveness of cancer models in mice. We do not expect the selected mouse cell lines to represent the variability present in patient populations. Further, cancer cells alter their phenotype in response to local microenvironments as they spread to metastatic sites. We measured changes in the expression of chemokines—signaling molecules that regulate cell homing and migration—as cancer cells spread from the primary tumor to lymph nodes and lungs (fig. S15). These data may provide clues as to how cancer cells can navigate from one metastatic site to another.

The route of cancer cell dissemination to distant sites in patients is complex and highly debated, in part due to limited clinical and experimental evidence. However, animal studies have linked large lymph node metastases to distant metastases (28). Further, studies using patient lymph node samples, human mammary carcinoma cells and xenograft tumors in immune-deficient mice have shown that cancer cells can invade lymphatic vessels in the sentinel lymph node and spread to additional nodes (29). Several clinical studies have also shown a relationship between the number of involved axillary lymph nodes and a higher risk for distant recurrence in breast cancer patients (13, 30, 31). Genetic studies examining the clonal relationships between cancer cells in the primary site, lymph nodes and distant organs have shown distant metastases are more closely related to lymph node metastases than to primary tumors in a subset of mice and patients (32, 33). Our mouse studies validate these data by directly showing that lymph node metastases can be a source of cancer cells for distant metastases. Our data are similar to results obtained independently by Brown *et al.*, using different methodologies in mouse models (34). Additionally, we have revealed that lymph node metastases can disseminate by invading lymph node blood vessels rather than by transiting through efferent lymphatic vessels. Further studies are needed to determine whether dissemination of cancer cells from lymph nodes is a feature of human cancer and, if so, whether it should be a factor in treatment decisions.

Supplementary Material

Refer to Web version on PubMed Central for supplementary material.

Acknowledgments

We thank R. K. Jain for critical discussion; S. Mordecai for assistance with imaging experiments; and K. Piatkevich for assistance with laser diodes. This work was supported by NIH grants DP2OD008780, R01CA214913, and R01HL128168 (TPP), NCI Federal Share/MGH Proton Beam Income-C06CA059267 (TPP), the Massachusetts General Hospital Executive Committee on Research ISF (TPP), NIH grant T32 DK007191 (DK), Susan G. Komen Foundation Fellowship PDF14301739 (GS), UNCF-Merck Science Initiative Postdoctoral Fellowship (DJ), Burroughs Wellcome Postdoctoral Enrichment Program Award (DJ), NIH NCI F32CA183465 (DJ), Korean MEST NRF-2012R1A1A2040866 (HJ), Samsung Biomedical Research Institute Grant GL1B22912 (HJ) and NIH P01CA080124. We thank M. Vangel and Harvard Catalyst, NIH Award UL1 TR001102 and financial contributions from Harvard University for assistance with biostatistical methods. ERP, DK and TPP conceived and designed experiments. ERP, DK, GS, OG, EFM, DJ, SMC, SK, EMB and EB performed experiments. ERP, GS, OG and TPP analyzed data. ERP, DK, GS, DJ, JC, HJ, MCC, AGT and TPP discussed results and strategy. TPP supervised the study. ERP and TPP wrote the manuscript, which was revised and approved by all authors.

References

1. Jatoi I, Hilsenbeck SG, Clark GM, Osborne CK. Significance of axillary lymph node metastasis in primary breast cancer. J Clin Oncol. 1999; 17:2334–2340. [PubMed: 10561295]
2. Kawada K, Taketo MM. Significance and mechanism of lymph node metastasis in cancer progression. Cancer research. 2011; 71:1214–1218. [PubMed: 21212413]
3. Ferris RL, Lotze MT, Leong SP, Hoon DS, Morton DL. Lymphatics, lymph nodes and the immune system: barriers and gateways for cancer spread. Clin Exp Metastasis. 2012; 29:729–736. [PubMed: 22851005]
4. Saksena MA, Saokar A, Harisinghani MG. Lymphotropic nanoparticle enhanced MR imaging (LNMRI) technique for lymph node imaging. Eur J Radiol. 2006; 58:367–374. [PubMed: 16472955]
5. Starz H, Balda BR, Kramer KU, Buchels H, Wang H. A micromorphometry-based concept for routine classification of sentinel lymph node metastases and its clinical relevance for patients with melanoma. Cancer. 2001; 91:2110–2121. [PubMed: 11391592]
6. Nathanson SD, Shah R, Rosso K. Sentinel lymph node metastases in cancer: causes, detection and their role in disease progression. Semin Cell Dev Biol. 2015; 38:106–116. [PubMed: 25444847]
7. Pereira ER, Jones D, Jung K, Padera TP. The lymph node microenvironment and its role in the progression of metastatic cancer. Semin Cell Dev Biol. 2015; 38:98–105. [PubMed: 25620792]
8. Cady B. Regional lymph node metastases; a singular manifestation of the process of clinical metastases in cancer: contemporary animal research and clinical reports suggest unifying concepts. Ann Surg Oncol. 2007; 14:1790–1800. [PubMed: 17342568]
9. Fisher B, et al. Twenty-five-year follow-up of a randomized trial comparing radical mastectomy, total mastectomy, and total mastectomy followed by irradiation. The New England journal of medicine. 2002; 347:567–575. [PubMed: 12192016]
10. Halsted WS. I. The Results of Radical Operations for the Cure of Carcinoma of the Breast. Annals of surgery. 1907; 46:1–19.
11. Cascinelli N, Morabito A, Santinami M, MacKie RM, Belli F. Immediate or delayed dissection of regional nodes in patients with melanoma of the trunk: a randomised trial. WHO Melanoma Programme. Lancet. 1998; 351:793–796. [PubMed: 9519951]
12. Nathanson SD, Kwon D, Kapke A, Alford SH, Chitale D. The role of lymph node metastasis in the systemic dissemination of breast cancer. Ann Surg Oncol. 2009; 16:3396–3405. [PubMed: 19657697]
13. Clarke M, et al. Effects of radiotherapy and of differences in the extent of surgery for early breast cancer on local recurrence and 15-year survival: an overview of the randomised trials. Lancet. 2005; 366:2087–2106. [PubMed: 16360786]
14. Morton DL, et al. Final trial report of sentinel-node biopsy versus nodal observation in melanoma. The New England journal of medicine. 2014; 370:599–609. [PubMed: 24521106]
15. Giuliano AE, et al. Axillary dissection vs no axillary dissection in women with invasive breast cancer and sentinel node metastasis: a randomized clinical trial. Jama. 2011; 305:569–575. [PubMed: 21304082]
16. Galimberti V, et al. Axillary dissection versus no axillary dissection in patients with sentinel-node micrometastases (IBCSG 23-01): a phase 3 randomised controlled trial. The Lancet Oncology. 2013; 14:297–305. [PubMed: 23491275]
17. Donker M, et al. Radiotherapy or surgery of the axilla after a positive sentinel node in breast cancer (EORTC 10981-22023 AMAROS): a randomised, multicentre, open-label, phase 3 non-inferiority trial. The Lancet Oncology. 2014; 15:1303–1310. [PubMed: 25439688]
18. Jagsi R, et al. Radiation field design in the ACOSOG Z0011 (Alliance) Trial. J Clin Oncol. 2014; 32:3600–3606. [PubMed: 25135994]
19. Faries MB, et al. Completion Dissection or Observation for Sentinel-Node Metastasis in Melanoma. The New England journal of medicine. 2017; 376:2211–2222. [PubMed: 28591523]
20. Poortmans PM, et al. Internal Mammary and Medial Supraclavicular Irradiation in Breast Cancer. The New England journal of medicine. 2015; 373:317–327. [PubMed: 26200978]

21. Whelan TJ, et al. Regional Nodal Irradiation in Early-Stage Breast Cancer. The New England journal of medicine. 2015; 373:307–316. [PubMed: 26200977]
22. Ly BH, Nguyen NP, Vinh-Hung V, Rapiti E, Vlastos G. Loco-regional treatment in metastatic breast cancer patients: is there a survival benefit? Breast Cancer Res Treat. 2010; 119:537–545. [PubMed: 19876731]
23. Punglia RS, Morrow M, Winer EP, Harris JR. Local therapy and survival in breast cancer. The New England journal of medicine. 2007; 356:2399–2405. [PubMed: 17554121]
24. Gurskaya NG, et al. Engineering of a monomeric green-to-red photoactivatable fluorescent protein induced by blue light. Nat Biotechnol. 2006; 24:461–465. [PubMed: 16550175]
25. Jeong HS, et al. Investigation of the Lack of Angiogenesis in the Formation of Lymph Node Metastases. J Natl Cancer Inst. 2015; 107
26. S JV, Gonzalez SF. Dynamic intravital imaging of cell-cell interactions in the lymph node. Journal of Allergy and Clinical Immunology. 2016; 139:12–20.
27. Chang JE, Turley SJ. Stromal infrastructure of the lymph node and coordination of immunity. Trends Immunol. 2015; 36:30–39. [PubMed: 25499856]
28. Crile G Jr, Isbister W, Deodhar SD. Demonstration that large metastases in lymph nodes disseminate cancer cells to blood and lungs. Cancer. 1971; 28:657. [PubMed: 5096929]
29. Kerjaschki D, et al. Lipoxygenase mediates invasion of intrametastatic lymphatic vessels and propagates lymph node metastasis of human mammary carcinoma xenografts in mouse. J Clin Invest. 2011; 121:2000–2012. [PubMed: 21540548]
30. Ragaz J, et al. Adjuvant radiotherapy and chemotherapy in node-positive premenopausal women with breast cancer. The New England journal of medicine. 1997; 337:956–962. [PubMed: 9309100]
31. Overgaard M, et al. Postoperative radiotherapy in high-risk premenopausal women with breast cancer who receive adjuvant chemotherapy. Danish Breast Cancer Cooperative Group 82b Trial. The New England journal of medicine. 1997; 337:949–955. [PubMed: 9395428]
32. McFadden DG, et al. Genetic and clonal dissection of murine small cell lung carcinoma progression by genome sequencing. Cell. 2014; 156:1298–1311. [PubMed: 24630729]
33. Naxerova K, et al. Origins of lymphatic and distant metastases in human colorectal cancer. Science. 2017; 357:55–60. [PubMed: 28684519]
34. Brown M, et al. Lymph node blood vessels provide exit routes for metastatic tumor cell dissemination in mice. Science. This issue.
35. Brown EB, et al. In vivo measurement of gene expression, angiogenesis and physiological function in tumors using multiphoton laser scanning microscopy. Nat Med. 2001; 7:864–8. [PubMed: 11433354]
36. Kedrin D, et al. Intravital imaging of metastatic behavior through a mammary imaging window. Nat Methods. 2008; 5:1019–21. [PubMed: 18997781]
37. Allinen M, et al. Molecular characterization of the tumor microenvironment in breast cancer. Cancer Cell. 2004; 6:17–32. [PubMed: 15261139]
38. Muller A, et al. Involvement of chemokine receptors in breast cancer metastasis. Nature. 2001; 410:50–56. [PubMed: 11242036]
39. Panse J, et al. Chemokine CXCL13 is overexpressed in the tumour tissue and in the peripheral blood of breast cancer patients. Br J Cancer. 2008; 99:930–938. [PubMed: 18781150]

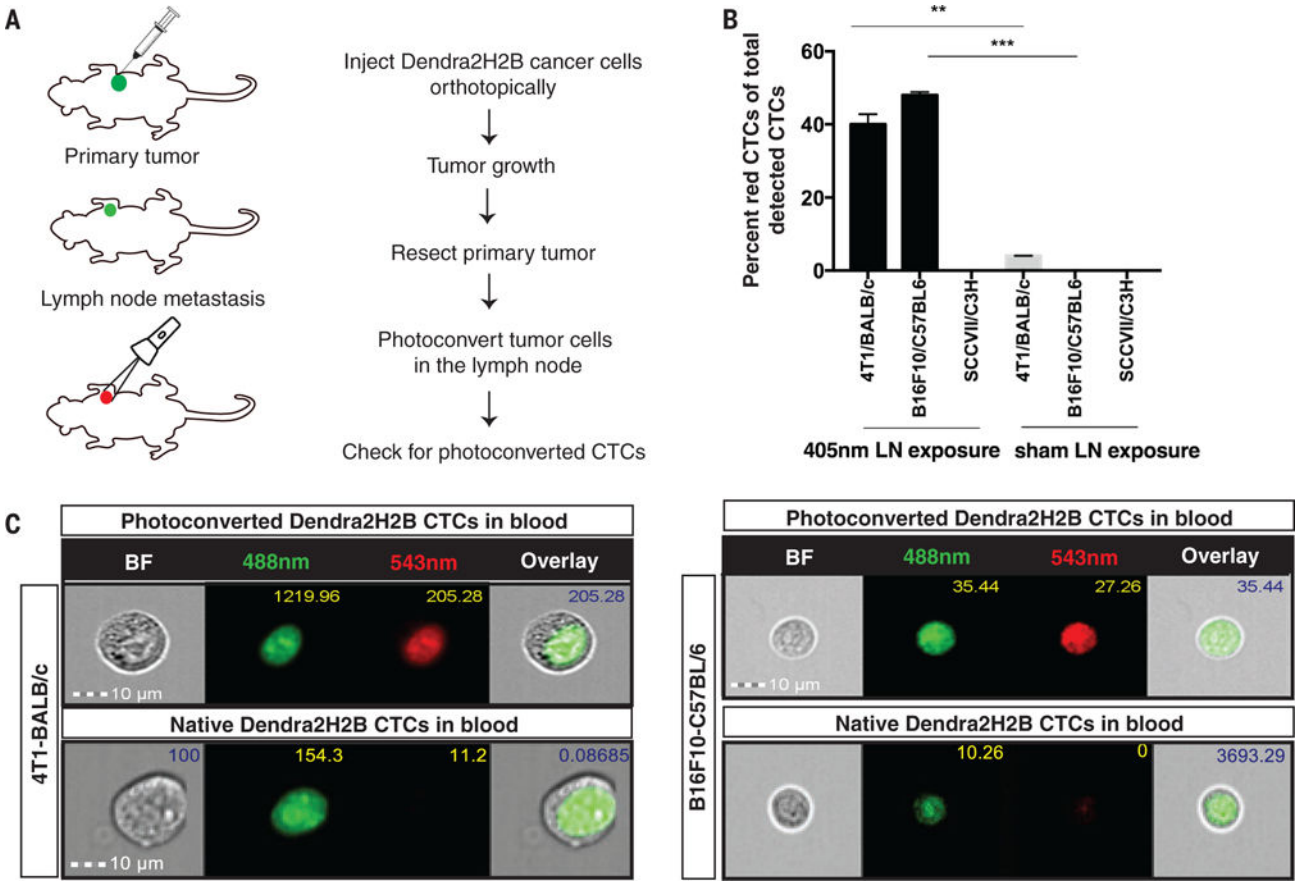

Fig. 1. Circulating tumor cells (CTCs) that transited through the lymph node detected in mouse models

(**A**) Dendra2H2B positive cancer cells were injected orthotopically into syngeneic recipients. Approximately 20 days later, the primary tumor was resected and tumor draining lymph nodes were photoconverted using a 405nm diode for 5 consecutive days. Blood was analyzed for the presence of green/red fluorescent CTCs using an Amnis Imagestream flow cytometer. (Photoconverted animals: 4T1 model n=11, B16F10 model n=7, SCCVII model n=5. Control animals: 4T1 model n=5, B16F10 model n=7, SCCVII n=3) (**B**) Dendra2H2B-4T1 cells and Dendra2H2B-B16F10 cells but not Dendra2H2B-SCCVII cells photoconverted in the draining lymph node were detected in the blood. Data are represented as the percentage of red CTCs (photoconverted) to total detected CTCs. Green CTCs were detected in all three models. *$p<0.05$ comparing 405nm light exposure to sham exposure for individual cells lines. (**C**) Representative images obtained by Imagestream of CTCs from 4T1/BALB/c and B16F10/C57BL/6 mouse models show positive photoconverted cancer cells verified by nuclear localization of Dendra2H2B. Scale bar=10µm.

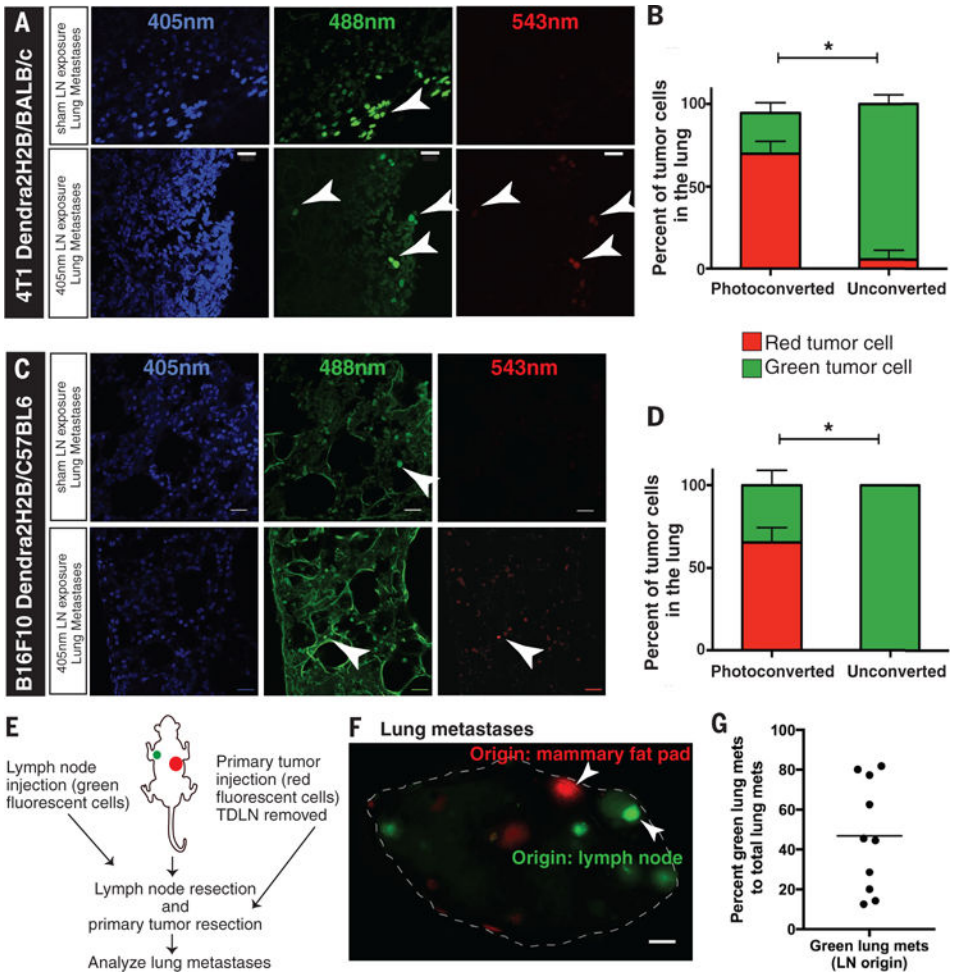

Fig. 2. Lymph node metastatic cancer cells can colonize the lung

(A, C) 100μm sections of fresh frozen lungs were obtained from Dendra2H2B-4T1 and Dendra2H2B-B16F10 tumor-bearing mice that either had their lymph node photoconverted with a 405nm diode or had no photoconversion. The top panels are representative images of micrometastatic disease (arrowheads) in the lung from control animals (no photoconversion), whereas the bottom panels show photoconverted isolated cancer cells that have colonized the lung via the lymph node. Scale bar=20μm. (**B, D**) The percentage of cancer cells detected in the lungs of Dendra2H2B-4T1 (n=8) and Dendra2H2B-B16F10 (n=8) tumor-bearing mice that were green (not photoconverted) versus red (photoconverted cells) are shown. *$p<0.05$ comparing 405nm light exposure (Photoconverted) to sham light exposure (Unconverted) for individual cells lines. (**E**) Schematic of experiment to determine whether cancer cells injected directly in the lymph node and in the mammary fat pad (MFP) can both form large metastases in the lungs. (**F**) Image of a lung with red lesions (originating from MFP) and green lesions (originating from lymph node) marked by arrowheads. Scale bar=1mm. (**G**) Lung metastases are represented as a percentage of lymph node origin metastasis (green) to total macroscopic lesions (red + green) (n=10). Using a one-sample Student's t-test, both lymph node and MFP origin tumors had an incidence greater than zero ($p<0.001$).

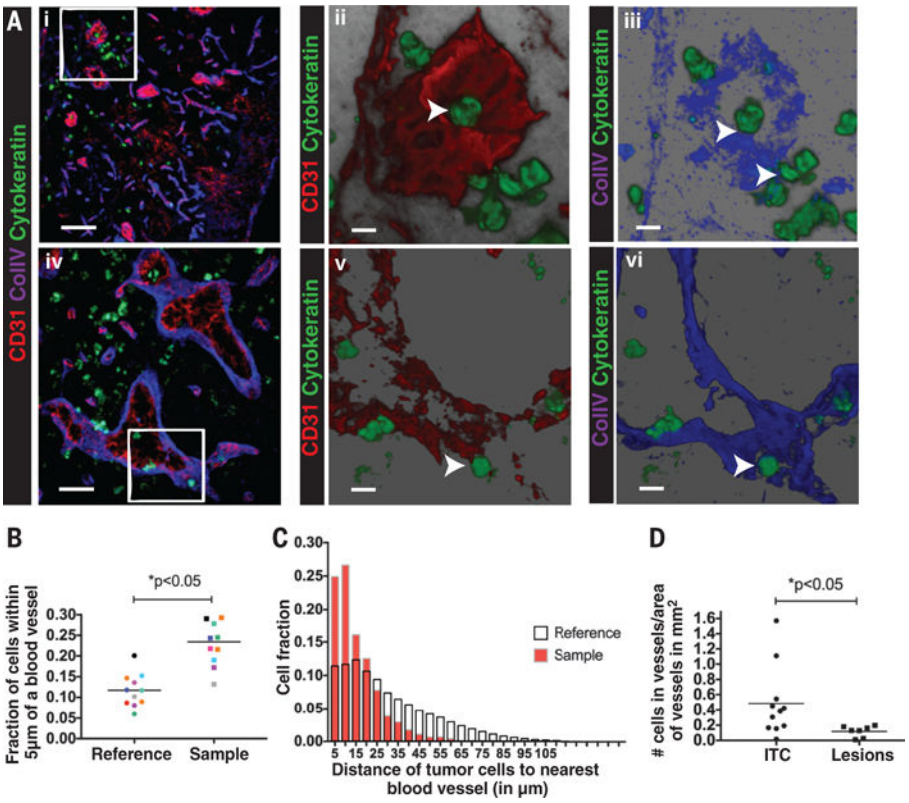

Fig. 3. Cancer cells in the lymph node associate with blood vessels and invade the vascular basement membrane

(**A**) (Ai, Aiv) Immunofluorescence staining of metastatic lymph nodes with isolated 4T1 cancer cells (anti-cytokeratin, green), blood vessels (anti-CD31, red) and basement membrane (anti- collagen IV, blue) shows cancer cells associating with blood vessels (Aii and Av, arrowheads) and the vascular basement membrane (Aiii and Avi, arrowheads). A cancer cell is observed inside a blood vessel (Aii and Aiii) (arrowhead). Scale bar= 50µm (Ai), 20µm (Aiv), 10µm (Aii,iii,v,vi) (**B**) Quantification of the fraction of cancer cells within 5µm of a blood vessel (Sample) in a lymph node compared to a theoretical random distribution (Reference) of the same number of cells in the same lymph node shows cancer cell association with lymph node blood vessels. n=11 individual lymph nodes *p<0.05. (**C**) Representative histogram of the fraction of cancer cells at varying distances from the nearest blood vessel in a given lymph node with isolated cancer cells (red bars-Sample) compared to the reference distribution for that lymph node (white bars-Reference). The measured distribution shows an association of cancer cells with blood vessels in the lymph node. (**D**) Quantification of the fraction of cancer cells inside a blood vessel in lymph nodes containing macro-metastatic lesions (Lesions) or isolated tumor cells (ITC).

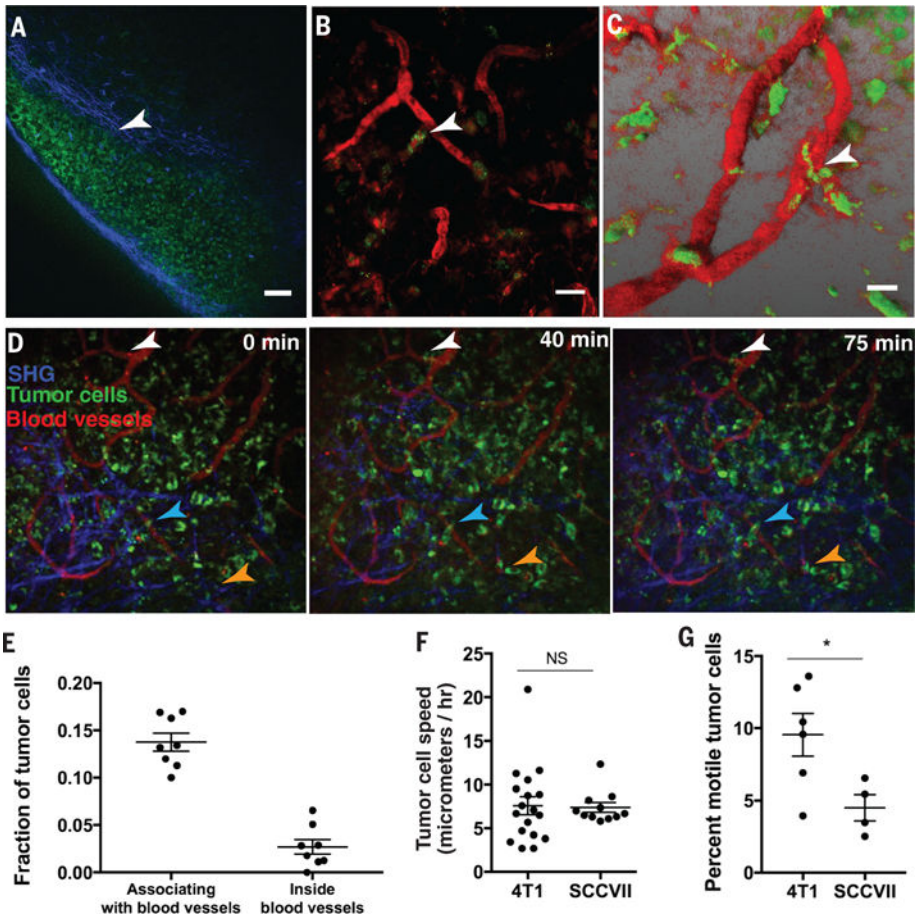

Fig. 4. Time-lapse intravital imaging of lymph node metastasis shows slow cancer cell migration toward blood vessels

(**A**) 4T1 Dendra2 expressing cancer cells (green fluorescence) form a large colony in the subcapsular sinus of the draining lymph node. Scale bar=60μm. (**B** to **C**) Cancer cells (green) that invaded the lymph node cortex wrapped around blood vessels (arrowheads), which were labeled by intravenous injection of rhodamine-dextran, 2million MW (red). Images were obtained by multiphoton microscopy at a depth of 80-110μm below the surface of the lymph node. Scale bar=20μm. (**D**) Time-lapse intravital imaging of cancer cells (green) in association with blood vessels (red) and collagen fibers (blue-detected by second harmonic generation) over the course of 75 min shows slow movement (arrowheads) of some cancer cells toward blood vessels. Images were obtained every 2 mins, with a 50μm z-stack. Scale bar=50μm. See also Supplementary Movies. (**E**) Quantification of the fraction of 4T1 tumor cells per field that associate with blood vessels or were inside blood vessels, analyzed by intravital microscopy in a tumor-draining lymph node. (**F**) Quantification of the speed of individual cancer cells in 4T1 and SCCVII lymph node metastases. (**G**) Quantification of the percentage of motile tumor cells in the image field over 75 min in 4T1 and SCCVII lymph node metastases. Quantification for (**E** to **G**) was done on 4-6 individual mice. Where indicated NS=not significant and *p<0.05.